

Electronic Supplementary Information (ESI)

Gold nanoclusters/MIL-100(Fe) bimodal nanovector for the therapy of inflammatory disease through attenuation of Toll-like receptor signaling

Heng Zhao,^a Sonia Becharef,^b Eddy Dumas,^c Florent Carn,^b Gilles Patriarche,^d Simona Mura,^e Florence Gazeau,^{*b} Christian Serre,^{*a} and Nathalie Steunou.^{*a,c}

a. Institut des Matériaux Poreux de Paris, ENS, ESPCI Paris, CNRS, PSL University, Paris, France. E-mail: christian.serre@ens.fr, nathalie.steunou@uvsq.fr

b. Université Paris Cité, MSC UMR CNRS 7057, 75006 Paris, France. E-mail: florence.gazeau@univ-paris-diderot.fr

c. Institut Lavoisier de Versailles, UMR CNRS 8180, Université de Versailles St Quentin en Yvelines, Université Paris Saclay, Versailles, France.

d. Université Paris-Saclay, CNRS, Centre de Nanosciences et de Nanotechnologies, 91120 Palaiseau, France.

e. Université Paris-Saclay, CNRS, Institut Galien Paris-Saclay, 91400, Orsay, France.

Table of Contents

Table of Contents	2
Experimental Section	3
Chemicals.....	3
Characterization techniques.....	3
Synthesis of MIL-100(Fe) Nanoparticles.	3
Synthesis of Au ₂₅ SG ₁₈ Nanoclusters (Au ₂₅ SG ₁₈ NCs).....	3
Synthesis of Au ₂₅ @MIL Nanoparticles.	4
Determination of the gold content.	4
Colloidal stability of Au ₂₅ (13)@MIL NPs.....	4
Encapsulation of dexamethasone phosphate (DexP) in Au ₂₅ (13)@MIL.....	4
Dexamethasone release of Au ₂₅ (13)@MIL/DexP.	4
Synthesis of Au ₂₅ (13)@MIL-HP or Au ₂₅ (13)@MIL/DexP-HP.	4
Figures and Tables	5
References.....	24

Experimental Section

Chemicals.

All chemicals were used as received without any further purification: iron(III) nitrate nonahydrate ($\text{Fe}(\text{NO}_3)_3 \cdot 9\text{H}_2\text{O}$, 98%), Dexamethasone 21-phosphate disodium salt, L-Glutathione reduced (GSH, >98%) and Potassium Chloride were purchased from Alfa Aesar. 1,3,5-benzenetricarboxylic acid (1,3,5-BTC, 95%), Lipopolysaccharides (LPS), 2',7'-Dichlorofluorescein Diacetate (DCF-DA), Hydrogen tetrachloroaurate(III) trihydrate ($\text{HAuCl}_4 \cdot 3\text{H}_2\text{O}$, $\geq 99.9\%$ trace metals basis), Hyaluronic acid (HA), Sodium borohydride (NaBH_4 , $\geq 98.0\%$), Dopamine hydrochloride (DA), Ammonium acetate and Potassium phosphate monobasic, Sodium chloride, phosphate buffered saline (PBS), Sodium phosphate monobasic dehydrate ($\text{NaH}_2\text{PO}_4 \cdot 2\text{H}_2\text{O}$) and Sodium phosphate, dibasic (Na_2HPO_4) were from Sigma-Aldrich. Cell counting kit-8 (CCK-8), were purchased from Dojindo. Propidium Iodide (PI), Pam3CSK4, QUANTI-Blue™, QUANTI-Luc™ and THP1-dual™ cells were purchased from InvivoGen. Hoechst33342 were purchased from Abcam. Proinflammatory cytokines (IL-1 β , IL-6 and TNF- α) DuoSet Elisa Kits and DuoSet ELISA Ancillary Reagent Kit 2 were purchased from R&D Systems. Acetonitrile, Methanol, Ethanol, Nitric acid (HNO_3 , 70%) and Hydrochloric Acid (HCl, 37%) unless specified and Sodium hydroxide (NaOH) were obtained from Fisher Chemical. Ultrapure water was obtained with the MilliQ purification system (Merck Millipore, France).

Characterization techniques.

Powder X-ray diffraction patterns (PXRD) were recorded on a high-throughput Bruker D8 Advance diffractometer working on transmission mode and equipped with a focusing Göbel mirror producing $\text{CuK}\alpha$ radiation ($\lambda = 1.5418 \text{ \AA}$) and a LynxEye detector. Thermogravimetric analyses (TGA) were performed on a Perkins Elmer SDA 6000 apparatus. Samples were heated up to 600 °C with a heating rate of 5 °C.min⁻¹ under an oxygen atmosphere. Transmission IR spectra were recorded in the 400-4000 cm⁻¹ range, with 4 cm⁻¹ resolution on a Nicolet Nexus spectrometer. N₂ sorption isotherms were obtained at 77 K using a Micromeritics Tristar instrument. Prior to the analysis, approximately 30 mg of samples were evacuated for 5 h at 120 °C under primary vacuum. Brunauer-Emmett-Teller (BET) surface and pore volume were estimated at a relative pressure lower than 0.25. TEM images were recorded on a JEOL 2010 TEM microscope operated at 200 kV. High resolution TEM images (HRTEM) were acquired on a Titan Themis 200 microscope operating at 200 kV. This microscope is equipped with a Ceta 16M hybrid camera from ThermoFischer Scientific capable of working under low electron irradiation conditions. The HRTEM images were obtained in low dose condition with an irradiation current between 100 and 250 electrons per square angstroms. High-angle annular dark field imaging in scanning transmission electron microscope mode (STEM-HAADF) images were acquired with a camera length of 110 mm (inner/outer collection angles were respectively 69 mrad and 200 mrad). Samples were prepared by deposition of one droplet of colloidal suspensions onto a carbon-coated copper grid and left to dry in air. ICP-MS was performed with an Agilent 7850 elemental analyzer. High Performance Liquid Chromatography (HPLC) analysis was performed by a Waters Alliance e2695 Separations Module (Waters, Milford, MA) equipped with a UV-Vis detector Waters 2998. A SunFire-C18 reverse-phase column (5 μm , 4.6 mm \times 150 mm, Waters) was employed. The particle diameter was measured by Dynamic Light Scattering (DLS) on a Zetasizer NanoZS (Malvern Instruments). Nanoparticles (NPs) (~0.1 - 0.2 mg·mL⁻¹) were dispersed at RT in aqueous solutions by using an ultrasound tip (Digital Sonifer 450, Branson) during 1 minute at 10% amplitude. Their surface charge was also evaluated by recording ζ -potential with the Zetasizer NanoZS.

Synthesis of MIL-100(Fe) Nanoparticles.

MIL-100(Fe) NPs were prepared according to the patent.¹ 0.72 g of $\text{Fe}(\text{NO}_3)_3 \cdot 9\text{H}_2\text{O}$ (1.78 mmol) was dissolved in 90 mL of distilled water. 0.25 g of 1,3,5-BTC (1.19 mmol) was then added to this solution and the suspension was allowed to stir for 48 h at room temperature (RT). The mixture was then centrifuged at 14500 rpm for 10 min. An orange solid was thus obtained. The as-synthesized MIL-100(Fe) NPs were then washed by two centrifugation/redispersion cycles in water followed by two centrifugation/redispersion cycles in absolute ethanol. The MIL-100(Fe) NPs were stored in EtOH and could be redispersed in water before use.

Synthesis of Au₂₅SG₁₈ Nanoclusters (Au₂₅SG₁₈ NCs).

Au₂₅SG₁₈ nanoclusters (NCs) were synthesized according to reported protocols.^{2,3} 2.0 mmol of GSH (614 mg) was added to a methanol solution of HAuCl_4 (50 mM, 100 mL). The mixture was then cooled to ~0 °C in a cool bath for 30 min. Then, a pre-cooled aqueous solution of NaBH_4 (0.2 M, 25 mL) was injected rapidly into this mixture under vigorous stirring. The mixture was allowed to react for another hour. The resulting precipitate was collected and washed repeatedly with methanol. Finally, the precipitate was dried in vacuum to obtain the Au:SG clusters as a dark-brown powder. Au:SG clusters were dissolved in an aqueous solution (14 mL) of GSH (130.7 mg), and the solution was stirred under an air at 328 K. After 3 h, the products were centrifuged to collect the supernatant, followed by dialysis with a molecular weight cut-off of 3000 Da in Milli Q water for 2 days and lyophilization.

Synthesis of Au₂₅@MIL Nanoparticles.

In the synthesis of Au₂₅@MIL NPs, a colloidal solution containing 10 or 50 mg of Au₂₅SG₁₈ NCs were added to 90 mL Fe(NO₃)₃·9H₂O (0.72 g, 1.78 mmol) aqueous solution under stirring. 0.25 g of 1,3,5-BTC (1.19 mmol) was then added and the mixture was stirred for 24 h at RT. The brown dark precipitate was centrifuged at 14500 rpm for 10 min. The solid was then washed by two centrifugation/redispersion cycles in water followed by two centrifugation/redispersion cycles in absolute ethanol. The Au₂₅@MIL NPs were stored in EtOH and could be redispersed in water before use. These Au₂₅@MIL NPs can be prepared by tuning the initial amount of Au₂₅SG₁₈ NCs (*i.e.* 10 or 50 mg of Au₂₅ NCs), leading to samples respectively labeled as Au₂₅(3)@MIL and Au₂₅(13)@MIL.

Determination of the gold content.

1 mg of Au₂₅(3)@MIL or Au₂₅(13)@MIL were accurately prepared and degraded with 1 mL of fresh aqua regia for 12 h, respectively. The solution was diluted by 2% HNO₃ solution for ICP MS analysis (Fe and gold ions). In parallel, 1 mg of Au₂₅(3)@MIL or Au₂₅(13)@MIL were treated with KOH and, after centrifugation (13400 rpm, 15min), BTC present in the supernatant (Fe ions precipitated) was then diluted using PBS and further quantified by HPLC. The mobile phase of HPLC is 50:50 v/v methanol : phosphate buffer (0.02 M NaH₂PO₄ and Na₂HPO₄, pH 2.5, adjusted by H₃PO₄). A flow rate of 0.8 mL/min and a sample injection volume of 25 µL were used during all analyses and UV detection was measured at 242 nm.

Colloidal stability of Au₂₅(13)@MIL NPs.

Au₂₅(13)@MIL NPs in EtOH were centrifuged and re-dispersed in different media: Milli Q water, 0.9% NaCl aqueous solution (Saline), PBS (pH 7.4, 10 mmol.L⁻¹), Dulbecco's Modified Eagle Medium (DMEM) and 90% DMEM + 10% fetal bovine serum (FBS) at a concentration of 200 µg/mL. After sonication (10 % amplitude for 30 seconds), the samples' hydrodynamic diameters were recorded over 3 experimental replicates. Furthermore, the long-time colloidal stability of Au₂₅(13)@MIL NPs in Mill Q water, PBS and DMEM + FBS was also studied by measuring the evolution of their hydrodynamic diameter with time. Values of diameter and Pdl were recorded at a period of 24 h (289 runs and 10 measurements per run and 30 seconds per measurement).

Encapsulation of dexamethasone phosphate (DexP) in Au₂₅(13)@MIL.

10 mg of Au₂₅(13)@MIL in Milli-Q water was mixed with 0.5 mL of DexP stock solution (10 mg/mL). The resulting suspension was stirred at 200 rpm at 25 °C for 24 h. The DexP loaded Au₂₅(13)@MIL nano-objects (*i.e.* Au₂₅(13)@MIL/DexP) were washed with Mill-Q water three times. The loading capacity of Au₂₅(13)@MIL/DexP was determined by HPLC. The mobile phase of HPLC is 50:50 v/v methanol: phosphate buffer (0.02 M NaH₂PO₄ and Na₂HPO₄, pH 2.5, adjusted by H₃PO₄). A flow rate of 0.8 mL/min and a sample injection volume of 25 µL were used during all analyses and UV detection was measured at 242 nm. The loading capacity (LC) or entrapment efficiency (EE) was calculated using the following equation:

$$LC = (\text{Mass of total drug} - \text{Mass of free drug}) / \text{Mass of total MOF}$$

$$EE = (\text{Mass of total drug} - \text{Mass of free drug}) / \text{Mass of total drug}$$

Dexamethasone release of Au₂₅(13)@MIL/DexP.

The cumulative release behaviour of DexP from Au₂₅(13)@MIL/DexP and Au₂₅(13)@MIL/DexP-HP (1 mg/mL, 1.5 mL) was investigated in PBS (pH=7.4) and PBS (pH=5.1) with or without 10 mM GSH for different incubation times (1 h, 4 h, 8 h, 24 h and 48 h). At different time intervals, the suspension of Au₂₅(13)@MIL/DexP or Au₂₅(13)@MIL/DexP-HP was centrifuged (13400 rpm, 15 min) and 0.5 mL of the release medium was replaced by the same volume of fresh medium. The concentration of released DexP and ligand 1,3,5-BTC was measured by HPLC.

Synthesis of Au₂₅(13)@MIL-HP or Au₂₅(13)@MIL/DexP-HP.

The hyaluronic acid-polydopamine (HA-PDA) copolymer was prepared according to the previously reported synthesis route.⁴ First, 1 g of hyaluronic acid (HA) was dissolved in 250 mL deionized water, then 0.52 g of sodium periodate was added. After stirring at RT for 24 h, aldehyde groups-bearing hyaluronic acid (HA-CHO) was obtained by dialysis and lyophilization. Then, 90 mg of HA-CHO and 462 mg of dopamine hydrochloride were dissolved in deionized water. The pH of the mixture was adjusted to 8.0 with diluted NaOH solution and the mixture was stirred at RT for 24 h. Similarly, after dialysis and lyophilization, the product was obtained. Au₂₅(13)@MIL-HP and Au₂₅(13)@MIL/DexP-HP NPs were prepared by mixing Au₂₅(13)@MIL and Au₂₅(13)@MIL/DexP solution respectively with HA-PDA solution at the weight ratio of 1:1 under stirring.

Figures and Tables

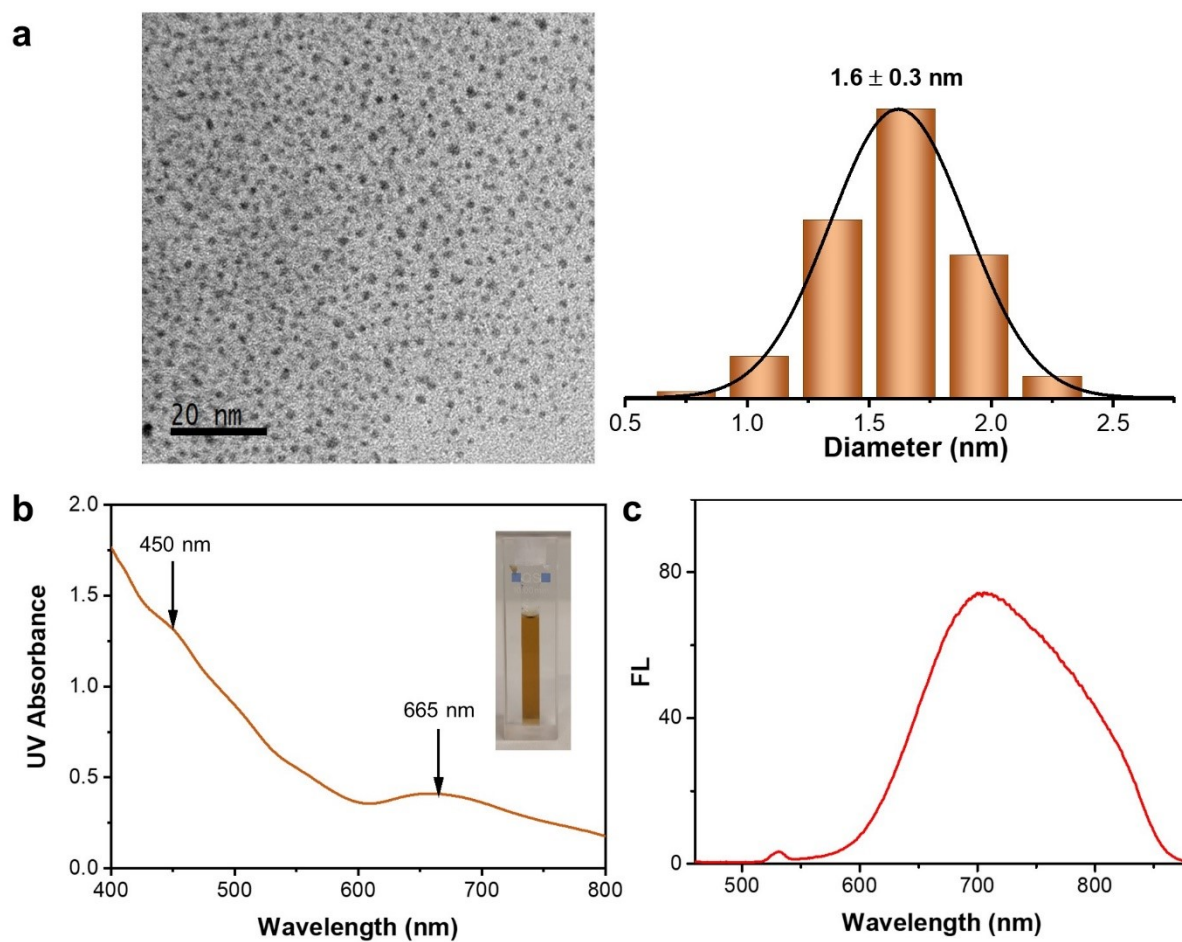


Fig. S1 a) TEM (statistical analysis figure inserted), b) UV-Vis and c) FL spectra of Au₂₅SG₁₈ NCs. The particle size distribution of Au₂₅SG₁₈ NCs was 1.6 ± 0.3 nm. Au₂₅SG₁₈ NCs exhibited two distinct absorption peaks at 450 and 665 nm associated with the Au 6sp intraband and interband transitions of bulk gold, respectively, which was consistent with previous literature.² The excitation wavelength used was 450 nm and the corresponding emission peak was ~700 nm.

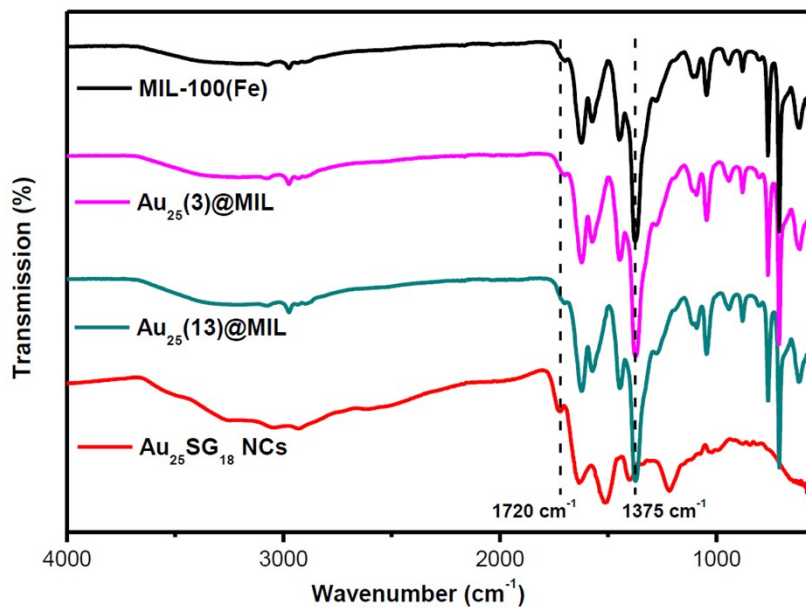


Fig. S2 FT-IR spectra of MIL-100(Fe), Au₂₅(3)@MIL, Au₂₅(13)@MIL and Au₂₅SG₁₈ NCs.

The sharp vibration bands at ~1624 and ~1375 cm⁻¹ are assigned to $\nu(\text{C-O})$ of carboxylate groups coordinated to the iron centers of the MOF. The weak band at ~1720 cm⁻¹ correspond to $\nu(\text{C-O})$ of carbonyl groups of GSH.

Table S1 Molar ratios of Au (ICP-MS) to Fe (ICP-MS) and BTC (HPLC) for Au₂₅(3)@MIL and Au₂₅(13)@MIL.

<i>Samples</i>	<i>Weight (mg)</i>	<i>ICP-Fe (μg)</i>	<i>ICP-Au (μg)</i>	<i>BTC (μg)</i>	<i>Fe : Au : BTC (molar ratio)</i>
Au ₂₅ (3)@MIL	1	135.4	6.5	422.5	100 : 1.4 : 83
Au ₂₅ (13)@MIL	1	121.3	33	368.5	100 : 7.7 : 80.7

This quantification could provide the X weight ratio of the Au₂₅(SG)₁₈ in the Au₂₅(X)@MIL composites (X= 3 and 13 wt%).

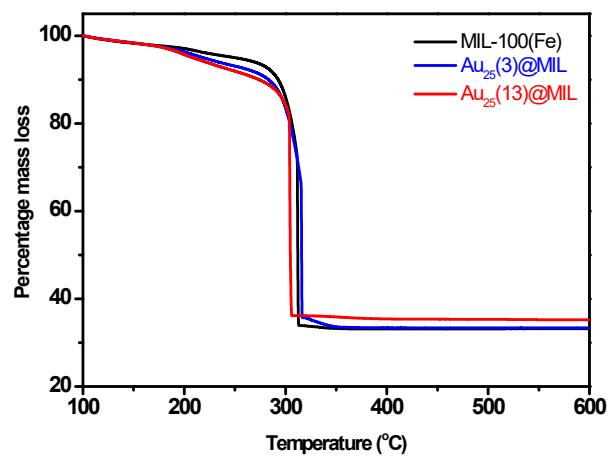


Fig. S3 TGA of MIL-100(Fe), Au₂₅(3)@MIL and Au₂₅(13)@MIL.

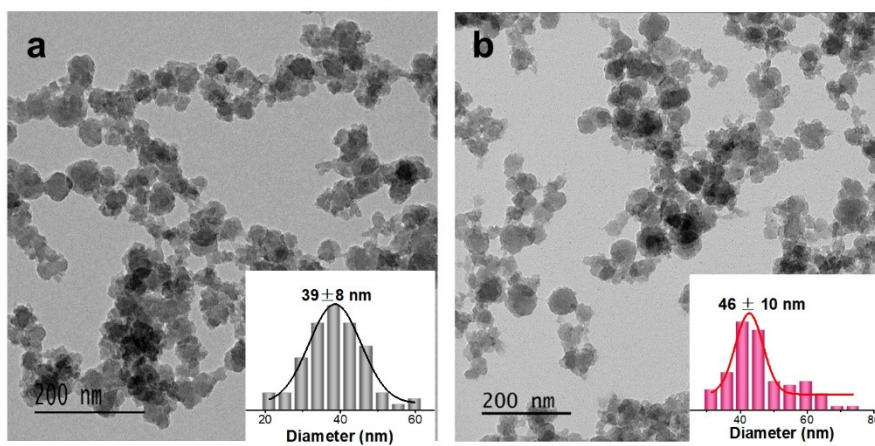


Fig. S4 TEM observations of (a) Au₂₅(3)@MIL and (b) Au₂₅(13)@MIL. The particle size distribution of Au₂₅(3)@MIL and Au₂₅(13)@MIL was 39 ± 8 nm and 46 ± 10 nm respectively.

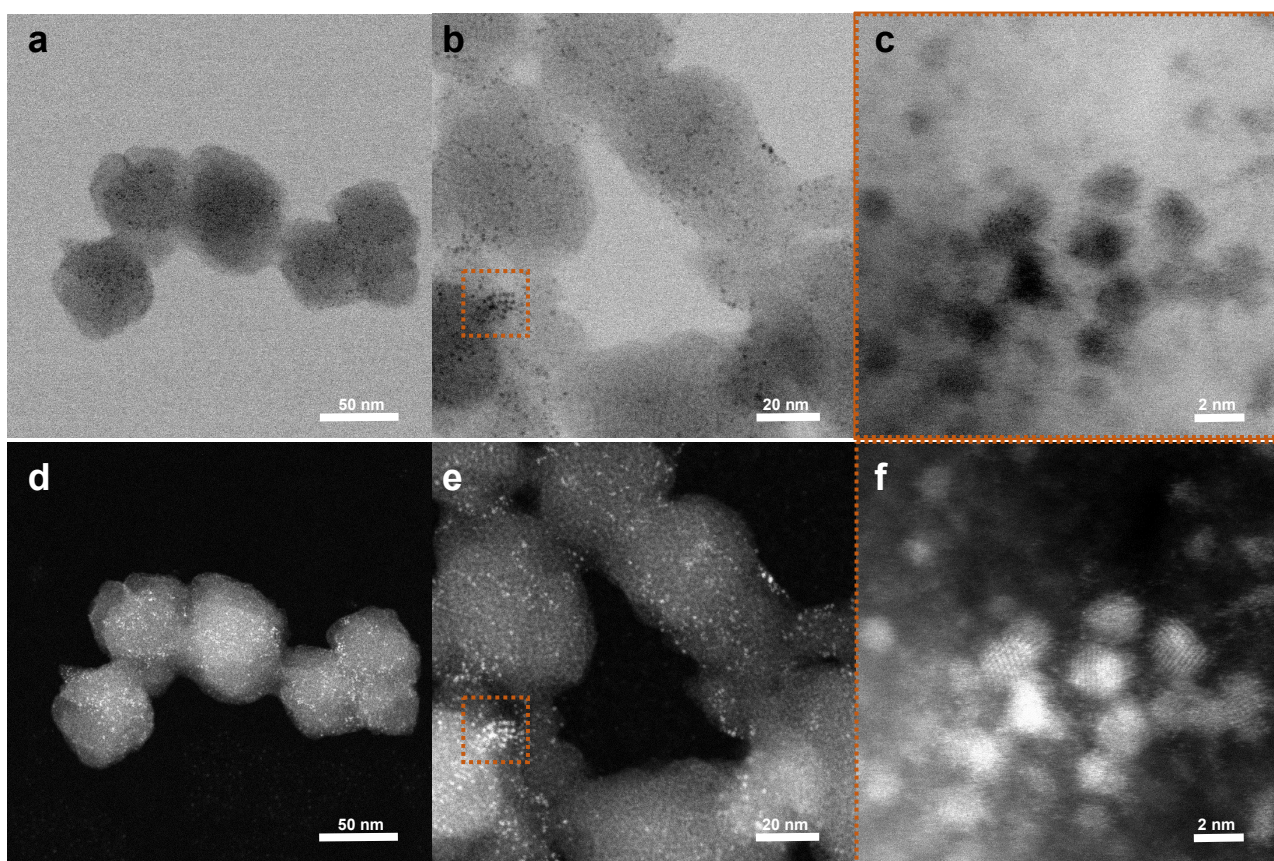


Fig. S5 a-c) TEM and d-f) STEM-HAADF of Au₂₅(3)@MIL. c) and f) images correspond to the area of b) and e) images visualized by dotted orange squares.

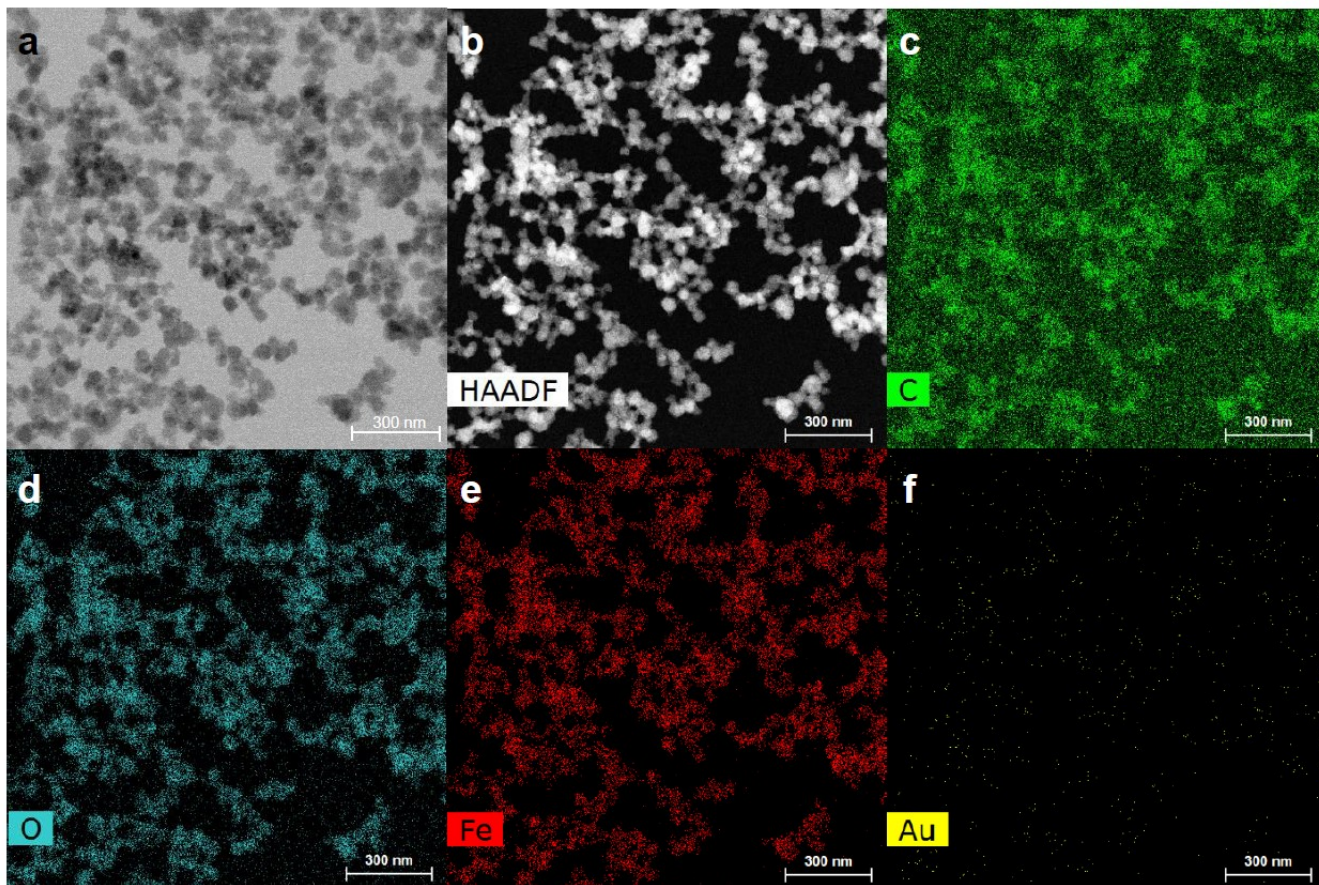


Fig. S6 a) TEM, b) STEM-HAADF and c-f) STEM-XEDS mapping images of $\text{Au}_{25}(3)\text{@MIL}$.

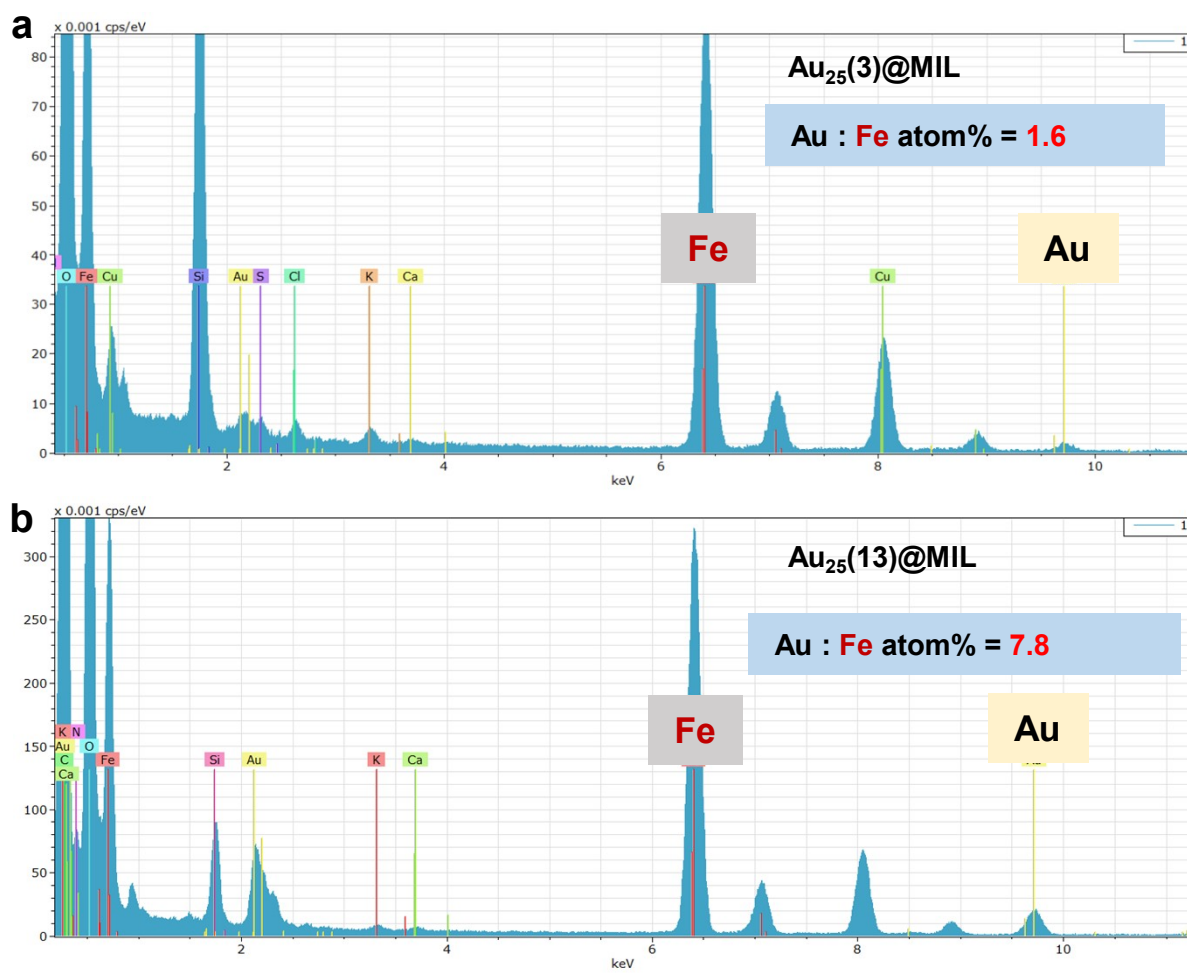


Fig. S7 XEDS of (a) Au₂₅(3)@MIL and (b) Au₂₅(13)@MIL. (Normalized atomic ratio between Au and Fe).

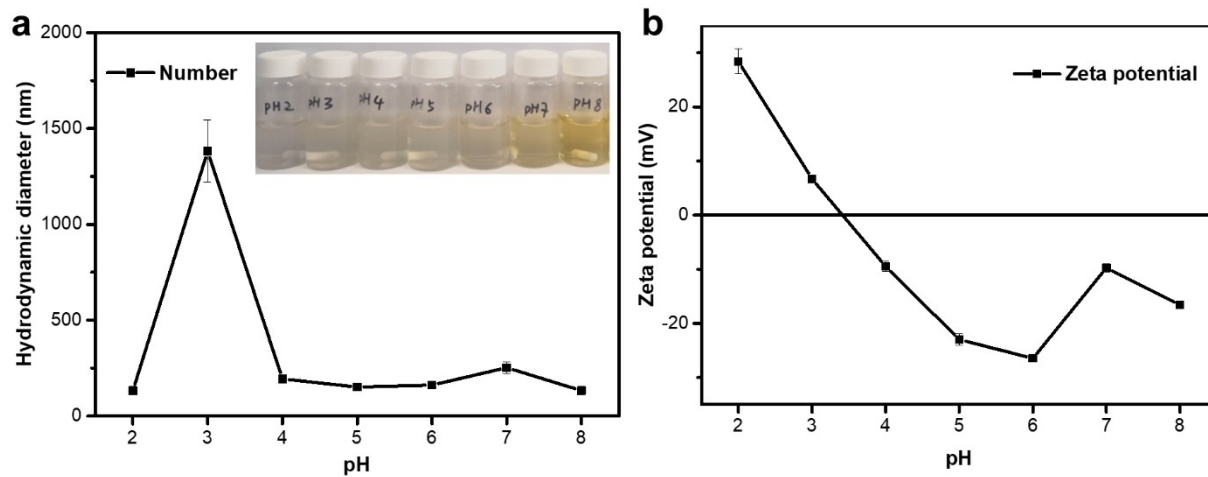


Fig. S8 a) pH dependent hydrodynamic diameters (by number) and (b) Zeta potential of Au₂₅(13)@MIL at a concentration of 100 μg/mL.

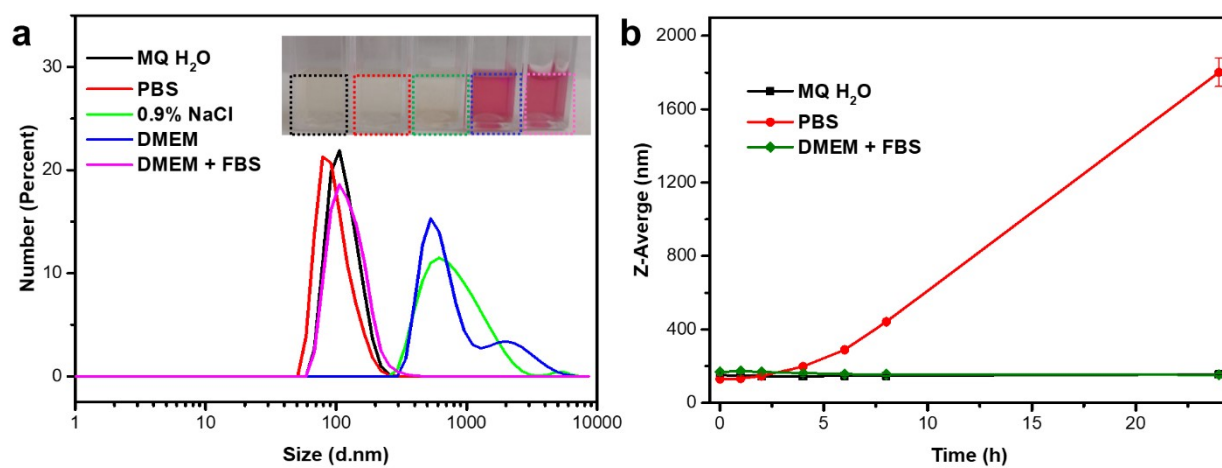


Fig. S9 A) The hydrodynamic diameters (by number) of Au₂₅(13)@MIL at a concentration of 100 μg/mL in different media (Milli Q water, PBS, 0.9% NaCl, DMEM and DMEM + FBS) at RT. B) Long term colloidal stability of Au₂₅(13)@MIL was conducted through monitoring evolution of the average particle diameter (by Z-Average) in Milli Q water, PBS and DMEM + FBS over 24 hours.

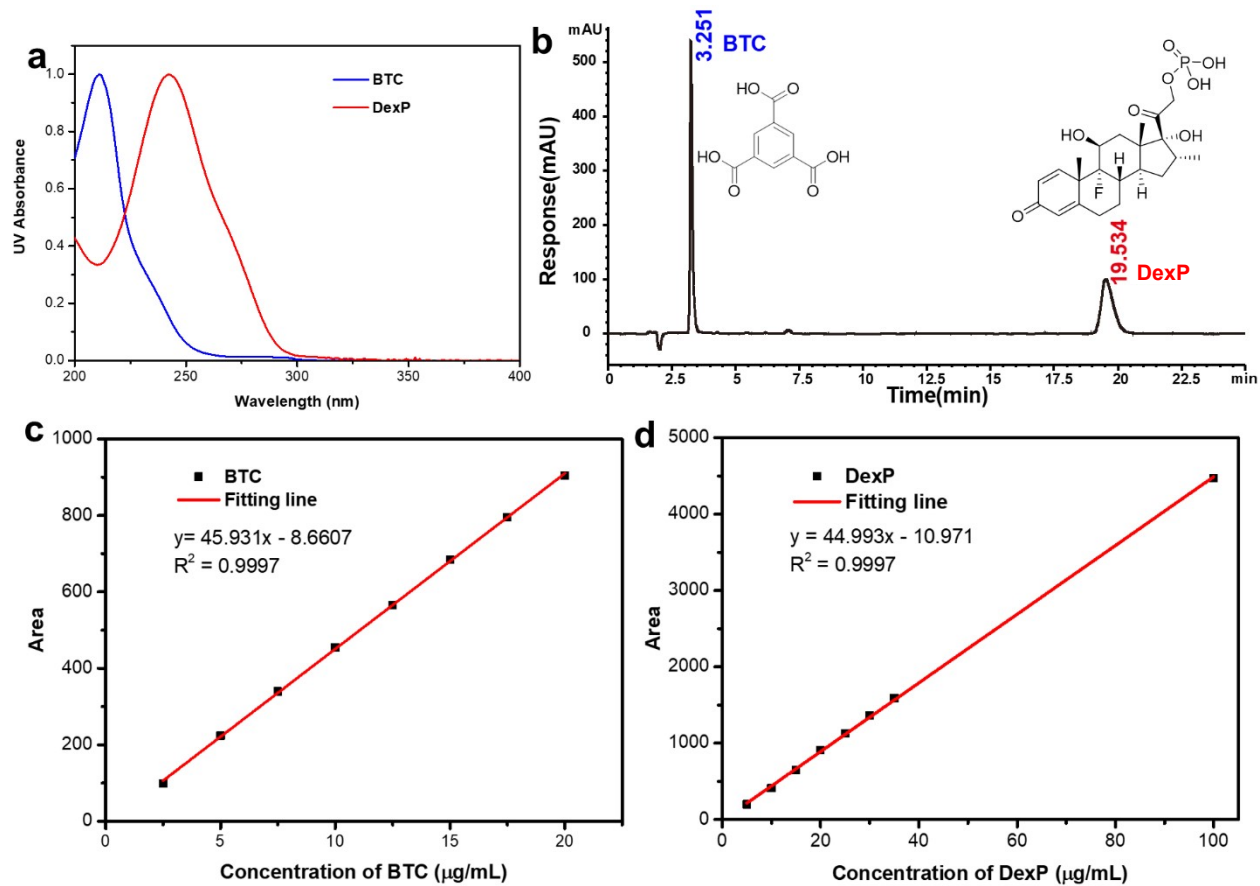


Fig. S10 a) UV-vis spectra and (b) HPLC chromatogram (Inserted: Molecular structure) of 1,3,5-BTC and DexP, (c, d) calibration curves of (c) 1,3,5-BTC and (d) DexP in water by HPLC.

Table S2 DexP loading capacity (LC) or entrapment efficiency (EE) of MIL-100(Fe) and Au₂₅(13)@MIL.

Weight Ratio (MOF : DexP)	MIL-100(Fe)/DexP LC (%)	MIL-100(Fe)/DexP EE (%)	Au₂₅(13)@MIL/DexP LC (%)	Au₂₅(13)@MIL/DexP EE (%)
1 : 0.5	49.1 ± 0.1	98.1 ± 0.3	43.3 ± 0.2	86.6 ± 0.4
1 : 1	60.4 ± 1.7	60.4 ± 1.7	46.6 ± 0.2	46.6 ± 0.2

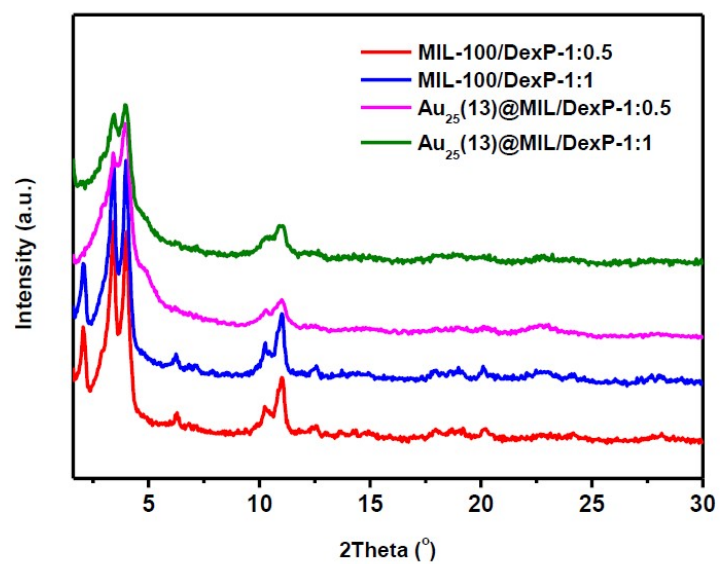


Fig. S11 PXR D patterns ($\lambda_{\text{Cu}}=1.5406 \text{ \AA}$) of MIL-100(Fe)/DexP and Au₂₅(13)@MIL/DexP. Au₂₅(13)@MIL/DexP was prepared with two different MOF/DexP weight ratio (1:0.5 and 1:1).

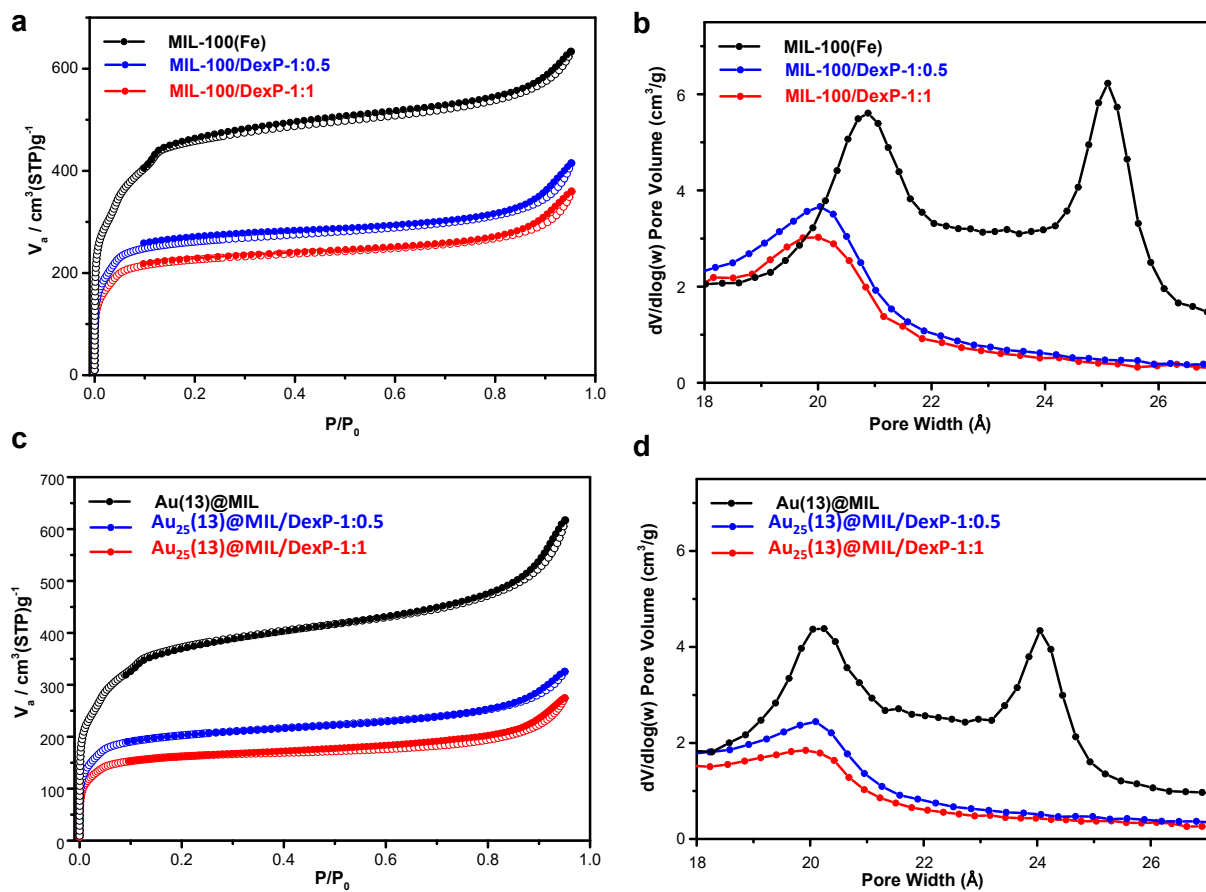


Fig. S12 a, c) Nitrogen sorption isotherms at 77 K ($P_0 = 1\text{atm}$) and corresponding (b, d) pore size distribution (PSD) derived from the Barrett–Joyner–Halenda (BJH) pore size model of MIL-100(Fe)/DexP and Au₂₅(13)@MIL/DexP. MIL-100/DexP and Au₂₅(13)@MIL/DexP were prepared with two different MOF/DexP weight ratio (1:0.5 and 1:1).

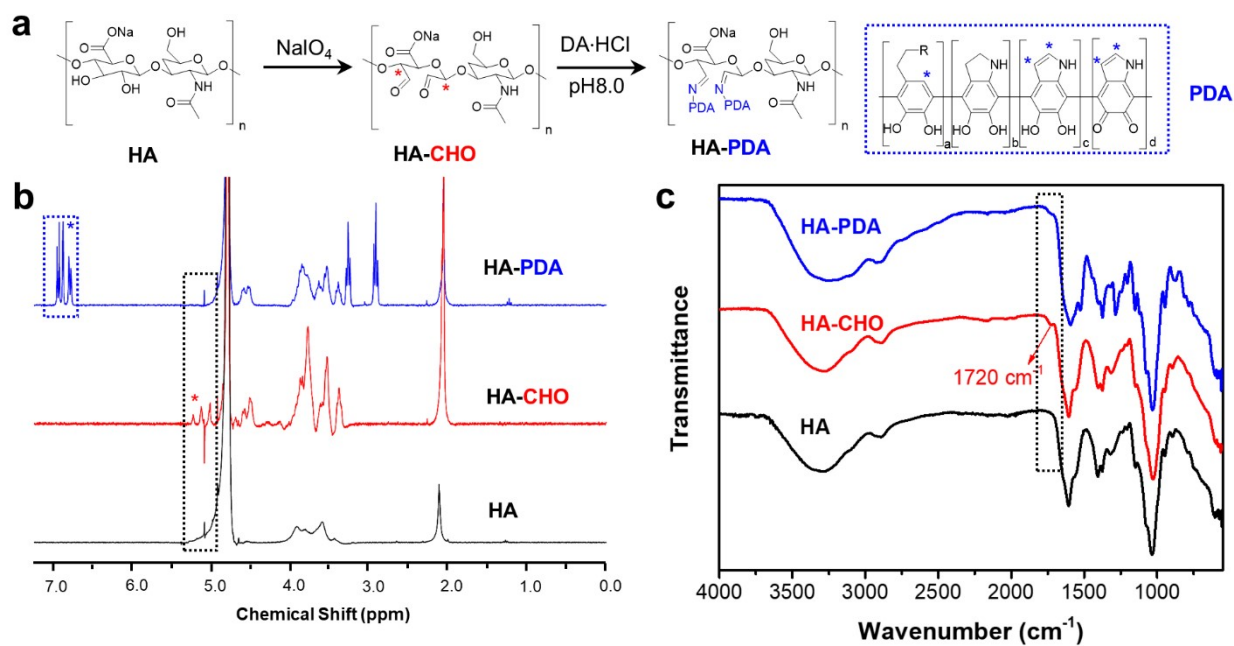


Fig. S13 Characterizations of HA-PDA. a) scheme of the reaction route of HA-PDA; b) ^1H NMR and c) FT-IR spectra of HA-PDA, HA-CHO and HA.

The characterization of HA-PDA by ^1H NMR and FT-IR was fully consistent with that previously reported.⁴

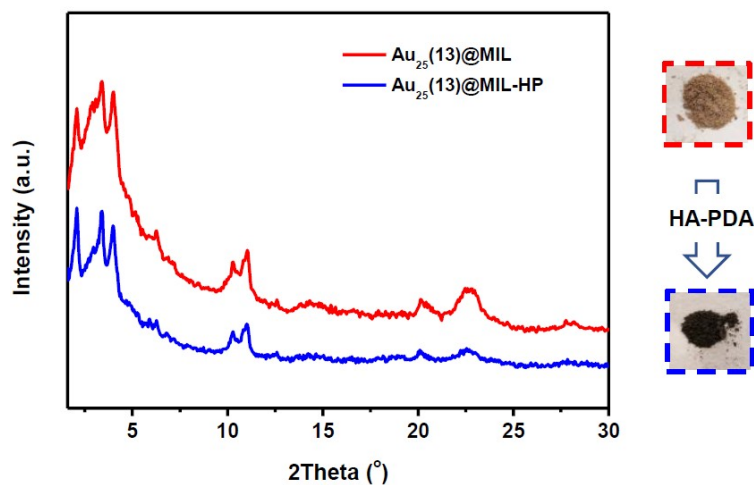


Fig. S14 PXRd patterns ($\lambda_{Cu}=1.5406 \text{ \AA}$) of $Au_{25}(13)@MIL$ and $Au_{25}(13)@MIL-HP$; Photographs before and after surface coating of $Au_{25}(13)@MIL$ by HA-PDA are shown.

After the surface modification of HA-PDA on $Au_{25}(13)@MIL$ (*i.e.* $Au_{25}(13)@MIL-HP$), the nano-object was characterized by PXRd and the crystalline structure of MIL-100(Fe) was preserved and meanwhile the color of the sample evolved from dark-brown to black

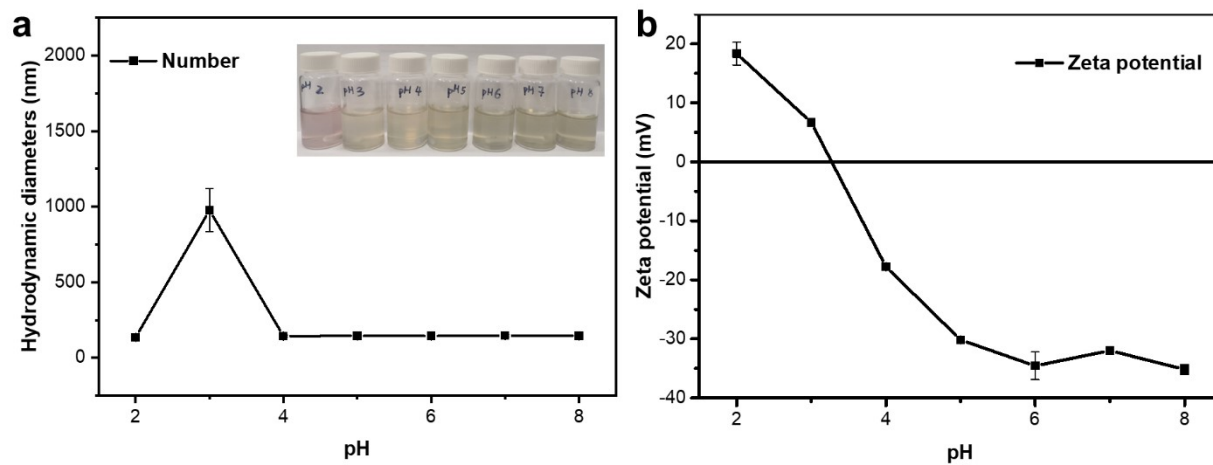


Fig. S15 a) Hydrodynamic diameter (by number) and (b) Zeta potential of Au₂₅(13)@MIL-HP as a function of pH.

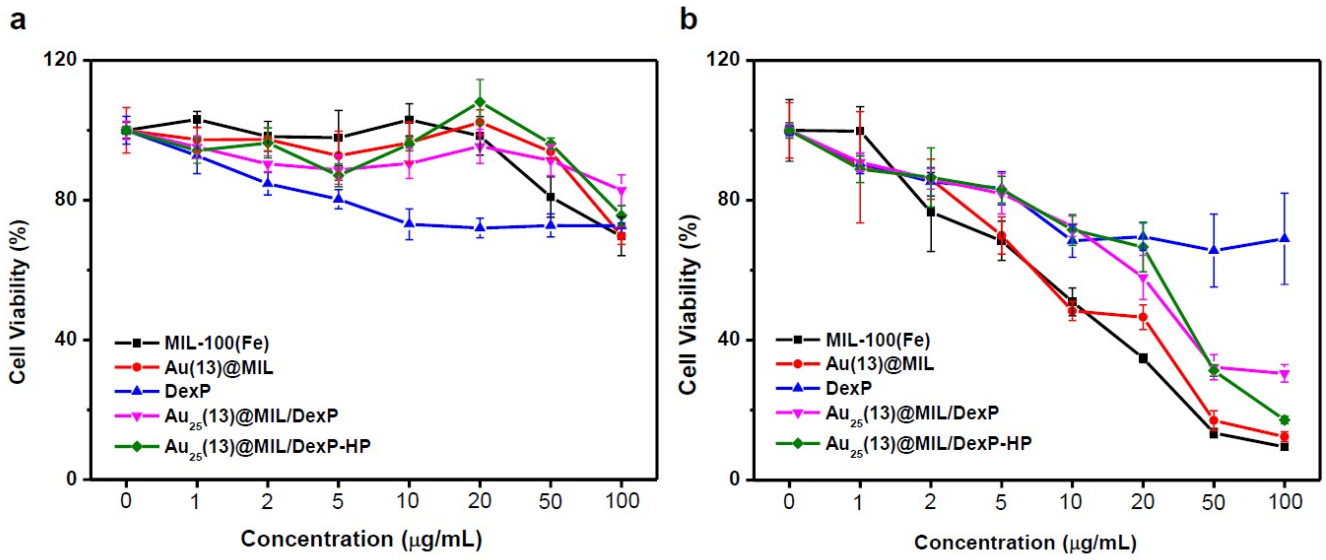


Fig. S16 Cell viability of (a) normal RAW264.7 macrophages and (b) LPS activated RAW 264.7 macrophages after incubation with different concentrations of MIL-100(Fe), Au₂₅(13)@MIL, DexP, Au₂₅(13)@MIL/DexP and Au₂₅(13)@MIL/DexP-HP for 24 hours. The experiments were performed in triplicate.

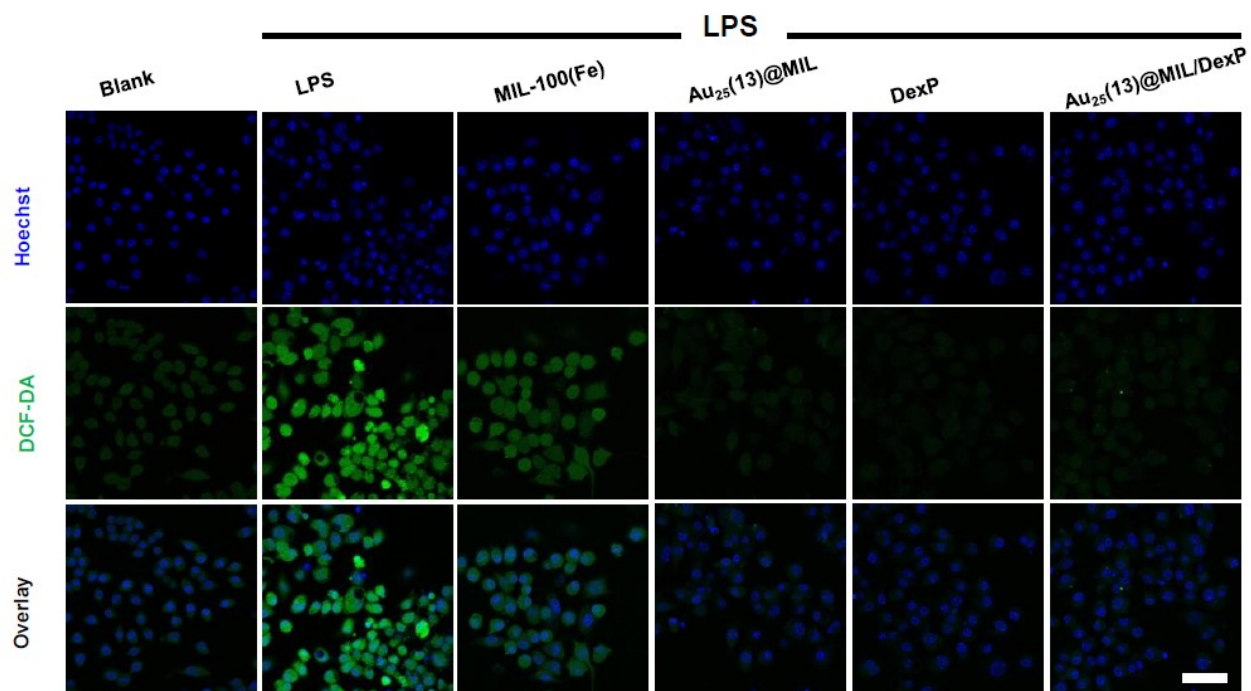


Fig. S17 Intracellular ROS imaging by using DCF-DA staining of RAW 264.7 macrophages incubated with MIL-100(Fe), Au₂₅(13)@MIL, DexP and Au₂₅(13)@MIL/DexP in the presence of LPS (100 ng mL⁻¹) for 24 h. Scale bar = 50 μm. The experiments were performed in triplicate.

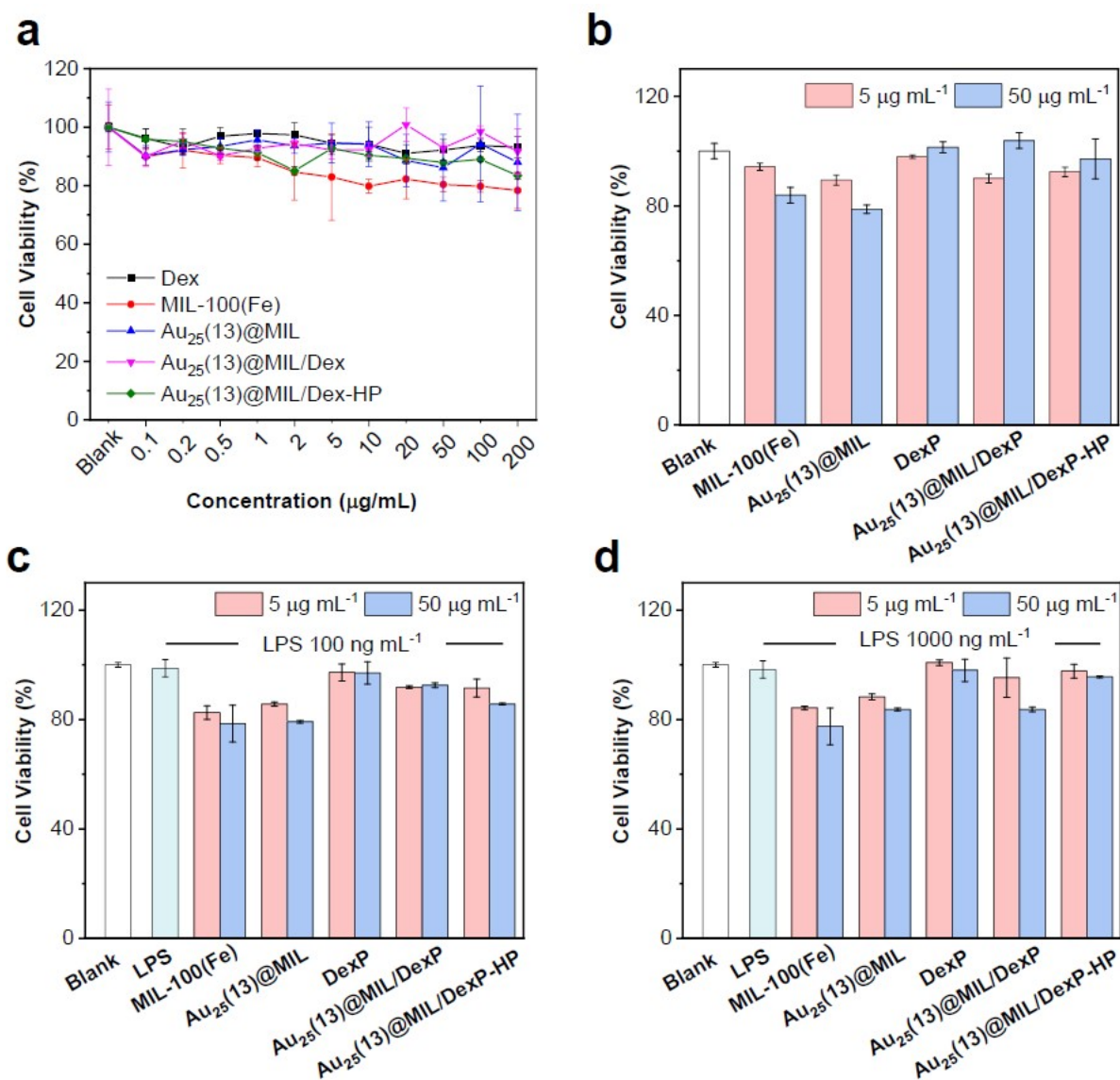


Fig. S18 The cell viability of (a, b) normal THP1-dual™ macrophage cells, and (c, d) THP1-dual™ macrophage cells treated with (c) 100 ng/mL and (d) 1000 ng/mL of LPS along with different formulations: MIL-100(Fe), Au₂₅(13)@MIL, DexP, Au₂₅(13)@MIL/DexP and Au₂₅(13)@MIL/DexP-HP at the concentration of (a) 0.1 to 200 µg.mL⁻¹ or (b-d) 5 or 50 µg.mL⁻¹ for 24 h. Cell viability assay was quantified by using CCK-8 kit. Results are shown as mean ± SD. The experiments were performed in triplicate.

References

- 1 M. Panchal, F. Nouar, C. Serre, M. Benzaqui, S. Sene, N. Steunou, M. Giménez Marqués, US Pat., 20210277042, 2021
- 2 Y. Negishi, K. Nobusada and T. Tsukuda, *J. Am. Chem. Soc.*, 2005, **127**, 5261-5270.
- 3 Y. Shichibu, Y. Negishi, H. Tsunoyama, M. Kanehara, T. Teranishi and T. Tsukuda, *Small*, 2007, **3**, 835-839.
- 4 Y. Zhang, L. Wang, L. Liu, L. Lin, F. Liu, Z. Xie, H. Tian and X. Chen, *ACS Appl. Mater. Interfaces*, 2018, **10**, 41035-41045.